Nanospace Decoration with Uranyl-Specific "Hooks" for Selective Uranium Extraction from Seawater with Ultrahigh Enrichment Index

Yanpei Song, Changjia Zhu, Qi Sun,* Briana Aguila, Carter W. Abney, Lukasz Wojtas, and Shengqian Ma*

ACCESS | Metrics & More | Article Recommendations | Supporting Information

ABSTRACT: Mining uranium from seawater is highly desirable for sustaining the increasing demand for nuclear fuel; however, access to this unparalleled reserve has been limited by competitive adsorption of a wide variety of concentrated competitors, especially vanadium. Herein, we report the creation of a series of uranyl-specific "hooks" and the decoration of them into the nanospace of porous organic polymers to afford uranium nanotraps for seawater uranium extraction. Manipulating the relative distances and angles of amidoxime moieties in the ligands enabled the creation of uranyl-specific "hooks" that feature ultrahigh affinity and selective sequestration of uranium with a distribution coefficient threefold higher compared to that of vanadium, overcoming the long-term challenge of the competing adsorption

of vanadium for uranium extraction from seawater. The optimized uranium nanotrap (2.5 mg) can extract more than one-third of the uranium in seawater (5 gallons), affording an enrichment index of 3836 and thus presenting a new benchmark for uranium adsorbent. Moreover, with improved selectivity, the uranium nanotraps could be regenerated using a mild base treatment. The synergistic combination of experimental and theoretical analyses in this study provides a mechanistic approach for optimizing the selectivity of chelators toward analytes of interest.
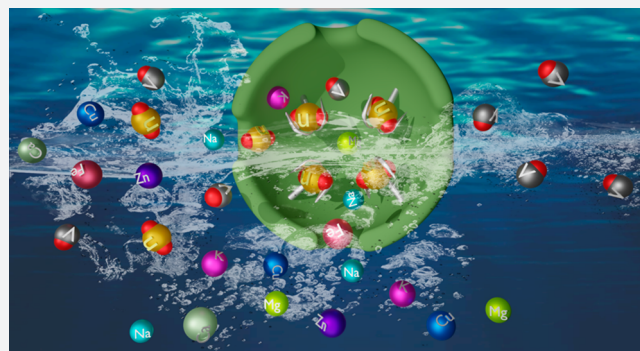
INTRODUCTION

The realization of net-zero CO_2 emissions by 2050, as advocated by the Paris Agreement, can help in stabilizing global warming below 2 °C to avoid pervasive climate damage. Significant efforts must be made in this regard to enable an energy revolution.[1−3] Among the numerous potential energy technologies, nuclear energy has proven to be a valid alternative to fossil fuels.[4−11] Uranium mining is essential to ensure long-term viability of nuclear power. Oceans are the Earth's largest reservoirs of uranium, which is more abundant in seawater than on land by several orders of magnitude; extracting this uranium can help in sustaining nuclear power production for millennia.[12−21] Efficient extraction of the potential uranium resources in seawater requires the use of highly selective sorbent materials for accumulating uranium. Although the development of efficient uranium adsorbents has been an elusive quest since the 1960s, its pace has slowed. Current adsorbents are generally insufficient to provide the selectivity required for recovering trace uranium species from numerous concentrated competing ions.[22−26]

Traditionally, the optimization of the selectivity of adsorbents has been mostly accomplished by designing new chelating sites, which are often accompanied by cumbersome synthetic procedures that hinder their practical applica-

tion.[27−29] The selective recognition and sequestration of specific ions occur efficiently in nature; this regulates the extreme selectivity for specific ions by manipulating the cooperation of binding sites. Therefore, approaches involving biomimetic designs have offered inspiration for designing sophisticated artificial materials.[30−36] Inspired by the preorganization of binding sites employed by nature, we previously demonstrated that the affinity of the chelating group in adsorbents toward uranium could be significantly improved by engineering their spatial distribution to facilitate cooperative binding.[37] Intrigued by this study, we sought to advance this strategy by creating uranyl-specific ligand "hooks" via precisely manipulating the relative distances and angles of chelators at the molecular level to alter the binding mode for enhanced metal selectivity. Given that amidoximes have been extensively studied and remain the premier adsorbents for uranium extraction from seawater, they were selected as the chelating

sites in the present study. However, the following constraints had to be considered: (i) the selectivity of amidoximes and their structurally related adsorbents toward uranium are hampered by their greater affinity toward vanadium, which is known to compete against uranium in the seawater extraction process; (ii) the binding between vanadium and the amidoxime moiety is strong, and separating them can cause irreversible damage during recycling, limiting their real-life implementation.[38−45] These deficiencies necessitate new strategies for improving the binding affinity of the amidoxime moiety toward uranyl ions.

Porous organic polymers (POPs) are highly topical classes of porous materials that are constructed by functional organic linkers; they feature large surface areas, functional diversity, structural flexibility, and exceptional stability. Therefore, POPs have shown tremendous promise for use in numerous applications and have exhibited encouraging outcomes.[46−52] Owing to their tunability, numerous strategies have been developed to enhance the binding of host−guest interactions, such as the introduction of noncovalent interactions and the manipulation of spatial distribution of chelators, which have been successful for designing various complexes with target selective recognition.[53,54] Previous crystallographic investigations have revealed that the modification of the R group in amidoxime-functionalized molecules can affect the coordination modes of U and V, thereby offering an opportunity to discriminate between the two and other competing ions in seawater.[55] Based on the promising results from this study, a series of diamidoxime ligands with various R groups were rationally designed as uranyl-specific "hooks" and decorated within the nanospace of porous organic polymers to afford uranium nanotraps (Scheme 1). In the present study, we

Scheme 1. Schematic Illustration of Nanospace Decoration of Uranium Nanotrap with Uranyl-Specific "Hooks" for Selective Capture of Uranium from Seawater
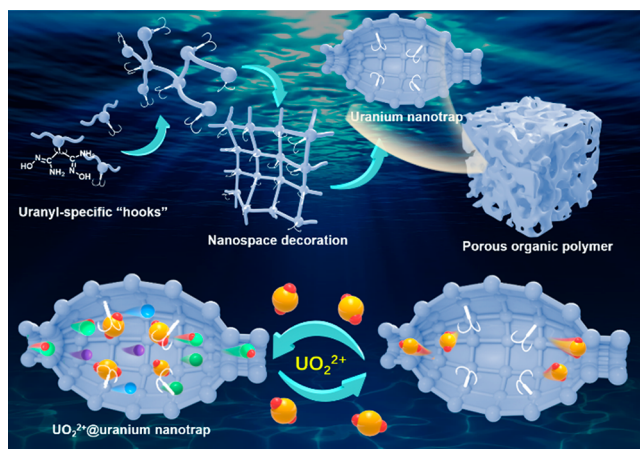
focused on the evaluation of the extraction of uranium over these uranium nanotraps with an emphasis on comparing their selectivity toward uranium and vanadium. Varying the R group in amidoxime was found to influence the binding affinity of amidoxime moieties to uranium and vanadium ions (Figure 1). These results open a new avenue for future research on improving the ion recognition ability of adsorbents.
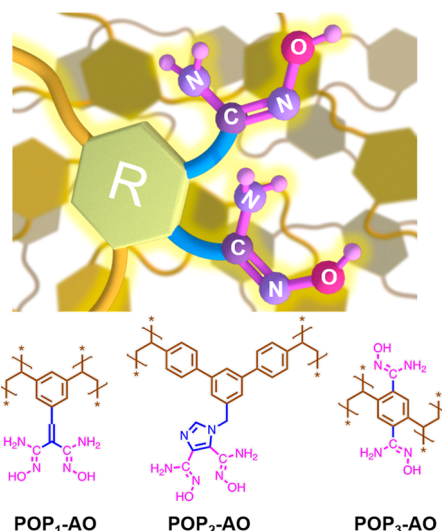

Figure 1. Porous frameworks constructed by uranyl-specific ligand "hooks" and the corresponding structures of diamidoxime-functionalized POPs investigated in this study.

■ RESULTS AND DISCUSSION

Materials Synthesis and Characterization. To prepare diamidoxime-functionalized POPs, vinyl-functionalized cyano compounds were first synthesized. The resulting compounds subsequently underwent free-radical polymerization with the yielded materials denoted as POP_1-CN, POP_2-CN, and POP_3-CN, which were further reacted with hydroxylamine to transform the cyano group into amidoxime (AO), yielding POP_1-AO, POP_2-AO, and POP_3-AO, respectively (Figure 1). Successful polymerization was indicated by the appearance of a strong peak at approximately 40 ppm in the solid-state ^{13}C nuclear magnetic resonance (NMR) spectra, which was attributed to the polymerized vinyl groups (Figures S1−S3).[56] The resulting POPs exhibited a combination of micro- and mesopores, as revealed by the N_2 sorption isotherms collected at 77 K, which showed a steep uptake at a relative pressure (P/P_0) of less than 0.1, accompanied by a hysteresis loop at relatively high pressures. The Brunauer−Emmett−Teller (BET) surface areas were calculated to be 585, 504, and 682 m^2 g^{-1} for POP_1-AO, POP_2-AO, and POP_3-AO, respectively (Figures S4−S6). Scanning electron microscopy (SEM) images revealed that these POPs contained aggregations of 50−100 nm-sized small particles, which further accumulated into macropores (Figures S7−S9). The meso- and macropores facilitated mass transfer, whereas the micropores served as traps that concentrate the chelating sites to enable a superior adsorption performance.[57,58] The appearance of the −C=N (1620 cm^{-1}), C−N (1370 cm^{-1}), and N−O (920 cm^{-1}) peaks, along with the disappearance of the −CN stretch (2220 cm^{-1}, Figures S10−S12), in the Fourier-transform infrared spectroscopy (FT-IR) profiles verified the transformation of −CN into amidoxime.[59] Furthermore, the diminishing intensity of the −CN peak at ∼110 ppm and the concomitant appearance of the characteristic peak of the amidoxime group at 170 ppm in the solid-state ^{13}C NMR spectra confirmed the high conversion efficiency enabled by the postsynthetic modification (Figures S1−S3).[60]

Uranium Sorption Studies. Upon the successful synthesis of diamidoxime functionalized POPs with various R groups, we first evaluated their uranium uptake capacities via batch
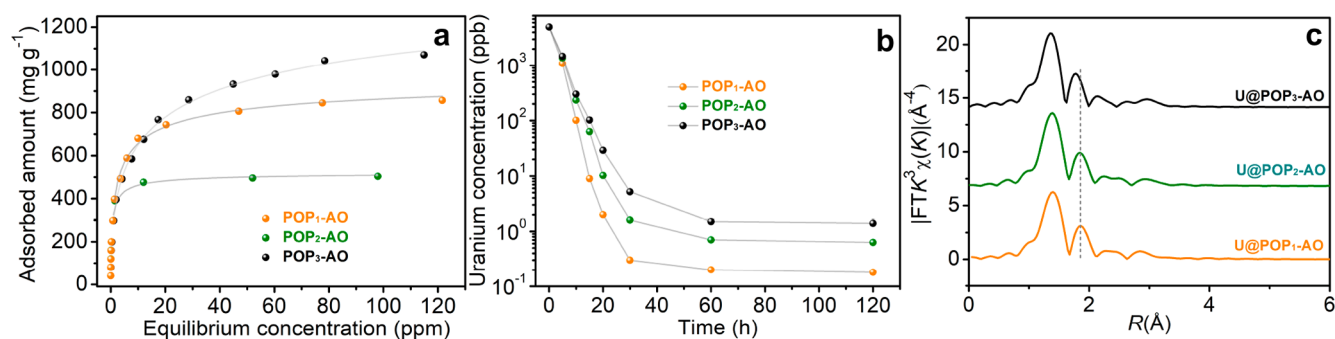
Figure 2. Uranium sorption performance evaluation and coordination environment investigation. (a) Uranium sorption isotherms for POP-based adsorbents. (b) The kinetics of uranium adsorption from aqueous solution with an initial concentration (5 ppm, 200 mL), at pH ~ 6, and sorbent material (5 mg). (c) A comparison of EXAFS spectra for U@POP$_1$-AO, U@POP$_2$-AO, and U@POP$_3$-AO.

adsorption experiments. Equilibrium uranium uptake capacity as a function of equilibrium uranium concentration by varying the initial uranyl concentrations from 20 to 700 ppm at pH ~ 6 (Figure S13) is displayed in Figure 2a. Both POP$_1$-AO and POP$_3$-AO exhibited higher uranium uptake capacities than POP$_2$-AO, which is reasonable given their higher density of amidoxime moieties compared to that in POP$_2$-AO. The equilibrium adsorption data were fit using the Langmuir model, providing an excellent description of the experimental values (Figures S14). The maximum uranium uptake capacities were estimated to be 857, 504, and 1070 mg uranium per gram of adsorbents for POP$_1$-AO, POP$_2$-AO, and POP$_3$-AO, respectively, at the equilibrium concentration of ~120 ppm.

Assuming that two amidoxime moieties coordinated with one UO_2^{2+} ion, the theoretical uranium uptake capacities for the POPs were calculated to be 875, 498, and 967 mg g^{-1} for OP$_1$-AO, POP$_2$-AO, and POP$_3$-AO, respectively. The comparable values between theoretical values and the experimental data indicated the full accessibility of amidoxime groups in the POPs. Notably, POP$_1$-AO exhibited steeper adsorption at low uranium concentrations than POP$_2$-AO and POP$_3$-AO, indicative of a stronger binding affinity of POP$_1$-AO toward uranium. Additionally, a dramatic color change from light yellow to red-orange was observed for POP$_1$-AO and POP$_2$-AO upon exposure to uranium solutions, while no obvious color change was observed for POP$_3$-AO, suggesting their differences in coordination fashion.

The kinetic efficiency of these sorbent materials was subsequently investigated to resolve these queries. Using 5 mg of the adsorbents in 200 mL of a 5-ppm uranium solution (pH = 6), 2 mL aliquots were drawn at appropriate time intervals to measure the content of uranium with time. All the investigated adsorbents were found to reduce the uranium species to less than 30 ppb (acceptable limit defined by the US Environmental Protection Agency for drinkable water) within 20 min with equilibrium concentrations of 0.18, 0.63, and 1.4 ppb corresponding to POP$_1$-AO, POP$_2$-AO, and POP$_3$-AO, respectively, after 2 h (Figure 2b). The resulting curves fit well with the pseudo-second-order kinetic model, which indicates chemisorption as the rate-determining step (Figure S15). Therefore, the discrepancy in sorption performance was primarily due to differences in complexing ability. The binding affinity of each adsorbent was quantified by calculating the distribution coefficient (K_d) at the equilibrium values. POP$_1$-AO (1.1×10^6 mL g^{-1}) was noted to exhibit the highest binding affinity toward uranium by an order of magnitude compared to that of POP$_2$-AO (3.2×10^5 mL g^{-1}) and POP$_3$-

AO (1.4×10^5 mL g^{-1}), which confirmed the effectiveness of varying the R group for designing efficient adsorbents.

X-ray photoelectron spectroscopy (XPS) profiles were collected to examine the uranium binding environments in the adsorbents. The appearance of strong U 4f signals in the tested adsorbents confirmed the presence of uranium. The complexation of uranium species with the adsorbents was indicated by the considerably lower binding energies of U 4f in these samples than those of pristine uranyl nitrate (Figure S16). To gain insight into the local coordination sphere of the uranium species, U K-edge extended X-ray absorption fine structure (EXAFS) spectroscopy was performed (Figure 2c). High-quality fits of the EXAFS data were obtained for uranium-loaded POP$_1$-AO and POP$_2$-AO through a qualitative comparison with a single crystal of uranyl with 4,5-diamidoxime imidazole. A fully cooperative chelating model was proposed for POP$_1$-AO and POP$_2$-AO because two amidoxime moieties coordinated with each uranyl ion and both oximates bounded in the η^2 (O, N) fashion, with the remaining equatorial plane being occupied by 1.6 ± 0.6 and 2 coordinating H$_2$O molecules, respectively. By contrast, POP$_3$-AO with chelating moieties at the opposite side featured only 1.8 ± 0.4 amidoxime ligands coordinated per UO_2^{2+}. This can be rationalized by the constraint that is imposed by the highly cross-linked polymer chains, which impedes the synergistic coordination of chelators from different monomers. This is further supported by the maximum uptake capacity values, which indicate that the amidoxime moieties in POP$_3$-AO bind to uranyl in a ratio of 1.7:1. Moreover, the EXAFS data of uranium including POP$_3$-AO (U@POP$_3$-AO) did not agree with the η^2-model fit, which validated different uranium binding modes in U@POP$_3$-AO compared to those in U@POP$_1$-AO and U@POP$_2$-AO.

Crystallographic and Density Functional Theory Calculation Studies. To provide more detailed structural insights into the molecular recognition behavior of these adsorbents, the corresponding small molecular ligands, **1**, **2**, and **3** for POP$_1$-AO, POP$_2$-AO, and POP$_3$-AO, respectively, were employed for complexation with uranyl. Single crystals of **2(UO$_2$)** and **3(UO$_2$)** were obtained via slow evaporation of the aqueous solutions of UO$_2$(NO$_3$)$_2$·6H$_2$O and the ligand, respectively; however, attempts to crystallize **1(UO$_2$)** suitable for X-ray crystallographic studies were unsuccessful. Notably, an immediate color change from yellow green to dark red-orange was observed upon the introduction of **2** to the aqueous uranyl solution. Single crystals of **2(UO$_2$)** were obtained in a dark reddish color, similar to that observed in the

color change of the adsorbents upon exposure to the uranium solution. X-ray structures of $2(UO_2)$ revealed that the ligand was dianionic. Both amidoxime and −OH groups were deprotonated and coordinated with uranyl in the η^2 fashion to yield a 1:1 complex with uranyl, which validated the EXAFS results. A zwitterionic tautomer containing four oxygen atoms from four oxime groups was found to bind to each uranyl in $3(UO_2)$ to form an infinite network, confirming the divergent binding modes in these adsorbents (Table S1). This difference was unanticipated; however, this emergent behavior that occurred due to the influence of the uranyl complexing mode could be a key contributor to the observed discrepancy in uranium sorption performance (Figure 3). To further
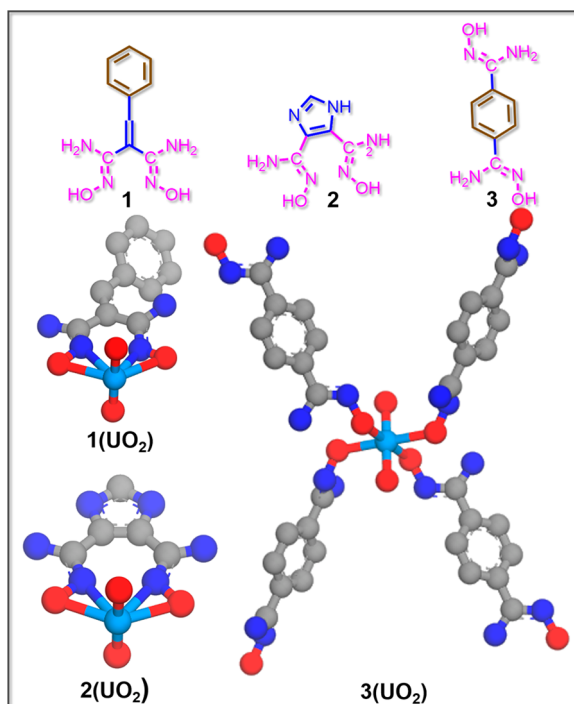

Figure 3. Structures of molecular ligands and the corresponding complexes with UO_2. The DFT optimized structure of $1(UO_2)$ and the single crystal structures of $2(UO_2)$ and $3(UO_2)$ (gray, C; blue, N; red, O; cyan, U; hydrogen is omitted for clarity).

uncover the reasons behind the distinctive uranium sorption performance, density functional theory (DFT) calculations were performed. The geometry-optimized structures are consistent with the experimentally determined structures, with complexation energies of 23.193, 22.261, and 18.253 eV

for $1(UO_2)$, $2(UO_2)$, and $3(UO_2)$, respectively, revealing a compact complex of **1** and uranyl ions. Based on the identical coordination modes in $1(UO_2)$ and $2(UO_2)$, the higher binding affinity of **1** toward uranium indicates the suitability of the binding pocket of **1** for uranyl ions, which is consistent with the experimental results (Figure S17). The present result could therefore point to a new approach involving the enhancement of the binding affinity, rather than designing new binding sites.

Selective Uranium Adsorption. Based on these characterization results, we subsequently focused on the selectivity of these adsorbents toward uranium in the presence of competitors prevalent in seawater. Given that the most important competitor in seawater uranium mining is vanadium, competitive adsorption experiments were performed by exposing the POPs to a binary mixture of uranium and vanadium solutions. Various adsorbents (5 mg) were stirred in a 200 mL solution with equal concentrations (50 ppm) of U and V for 2 h. A reduced uranium concentration from 50 to 36.1 ppm was detected for the solution treated with POP_1-AO, whereas the uranium concentrations leftover upon treatment with POP_2-AO and POP_3-AO were 43.6 and 44.1 ppm, respectively. To quantify the impact of vanadium on uranium adsorption, the reduction rate of uranium uptake capacity was evaluated, which revealed that 65, 51, and 22% uptake capacities were exhibited by POP_1-AO, POP_2-AO, and POP_3-AO, respectively (Figure 4a). Based on these results, POP_1-AO was confirmed to possess superior binding characteristics for uranium over vanadium. Calculation of the K_d values for uranium and vanadium revealed that the K_d value of POP_1-AO for uranium was more than three times greater than that for vanadium (Figure 4b). By contrast, POP_2-AO showed comparable K_d values for uranium and vanadium, and POP_3-AO exhibited a higher binding affinity toward vanadium than that for uranium (see detailed summary in Table S2). To further support the high affinity of POP_1-AO toward uranium than that of vanadium, we evaluated its sorption performance in the presence of equal molar concentrations of vanadium (0.22 mM, 11 ppm) and uranium (0.22 mM, 50 ppm), showing a uranium uptake capacity of 2.966 mmol g^{-1} (or 706 mg g^{-1}), which is substantially larger than that of V (0.628 mmol g^{-1} or 32 mg g^{-1}).

The ability to completely recover and recycle adsorbents is crucial for their real-world application, which also justifies the high costs of sorbent materials. Therefore, the reacted adsorbents were eluted using a 0.1 M Na_2CO_3 solution to probe this aspect. The performance of POP_1-AO was maintained for ten consecutive cycles, demonstrating its excellent stability and reusability. However, the treatment of
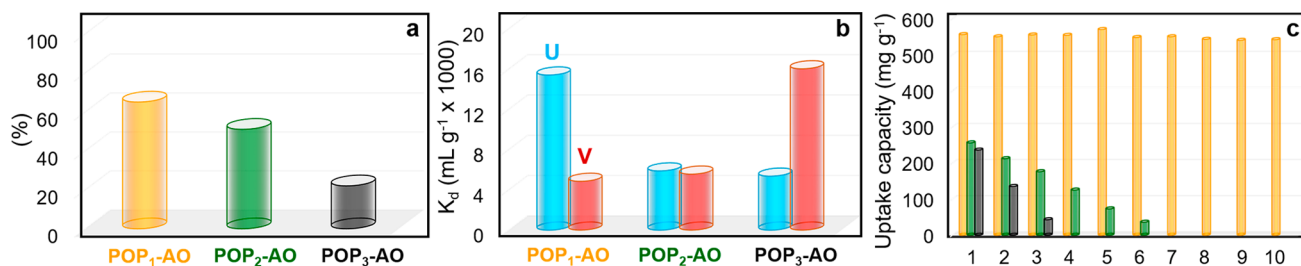

Figure 4. Selectivity and recyclability evaluation. (a) The remaining uranium uptake capacity of various sorbent materials in the presence of equal concentration of vanadium. (b) The K_d values for uranium and vanadium over various sorbent materials (cyan, uranium; red, vanadium). (c) The recyclability of various reacted sorbent materials after treatment with Na_2CO_3 (orange, POP_1-AO; olive, POP_2-AO; black, POP_3-AO).

reacted POP_2-AO and POP_3-AO with Na_2CO_3 failed to fully release the bound metal species, as inferred from the decreased uptake performance (Figure 4c). To rationalize this phenomenon, the complexation of uranium and vanadium with the Na_2CO_3-treated loaded POP_2-AO and POP_3-AO was investigated using XPS (Figure S18). Discernable vanadium peaks were observed for the loaded POP_2-AO and POP_3-AO, suggesting the ineffectiveness of the regeneration process and insufficiency of the selectivity. The effective regeneration of POP_2-AO and POP_3-AO was achieved by stirring in HNO_3 (1 M). However, consecutive cycles revealed that the regenerated samples showed noticeably decreased performance, and only 87 and 77% of their initial capacities were retained by POP_2-AO and POP_3-AO, respectively. These experiments revealed that the modification of the R group enabled the selective discrimination of amidoxime moieties toward uranium compared to other metal species.

To further evaluate the reliability of the proposed strategy, uranium adsorption was investigated using a large excess of Na^+, K^+, Mg^{2+}, Zn^{2+}, Cu^{2+}, Fe^{3+}, and Ca^{2+} (100 ppm each); these ions were selected to facilitate competition against uranium in these extraction experiments and because of their abundance in natural seawater streams. Under competitive adsorption conditions, POP_1-AO almost completely removed uranium, and reduced the uranium content from 5 ppm to 0.43 ppb, while more than 98.4% of other ions remained in the solution (Tables S3 and S4). Meanwhile, POP_2-AO and POP_3-AO exhibited a decreased capacity and reduced the concentration to only 4.8 and 11.5 ppb, respectively; this confirmed that POP_1-AO formed a more stable complex with uranium.

Uranium Capture from Natural Seawater. To assess the potential utility of these adsorbents for seawater uranium extraction, large-scale adsorption experiments were conducted in an effort to accurately depict the uranium uptake capacity by ensuring that an excess of uranium was present. Experiments were conducted by introducing 2.5 mg of sorbent materials into 5 gallons of seawater collected from the coast of Broad Key, United States. After 56 days of contact, the loaded sorbent materials were collected and the enriched uranium species was eluted with aqua regia, affording values of 8.4, 5.5, and 3.1 mg of uranium per gram of adsorbent for POP_1-AO, POP_2-AO, and POP_1-AO, respectively, indicating that more than one-third of the uranium dissolved in the seawater can be enriched by POP_1-AO. Notably, the enrichment index of the uranium for POP_1-AO was calculated to be 3836, which is considerably close to the all-time seawater uranium accumulation record (see the summary of the reported representative adsorbents in uranium uptake capacity, selectivity of uranium and vanadium, seawater uranium uptake capacity, and the enrichment index in Tables S5 and S6).

CONCLUSION

A family of uranyl-specific diamidoxime ligand "hooks" was constructed into porous frameworks and systematically investigated to evaluate their uranium-capturing properties and to overcome the challenge involving competitive adsorption of vanadium. The strategy essentially involved modification of the R group to manipulate the cooperation of binding sites and to eventually enhance the selective recognition of the resulting adsorbents toward uranium against other ions. Experimental evidence confirmed that the actual active binding sites for the sequestration of uranium from seawater involved the amidoxime groups located at appropriate positions, which enabled cooperative binding in the adsorbents and increased the density of adjacent amidoxime groups. This strategy can possibly constitute a general design principle for the further development of efficient adsorbents. More broadly, this study can be a valuable starting point to guide further development of efficient adsorbents to extract useful resources from seawater.

ASSOCIATED CONTENT

SI Supporting Information

The Supporting Information is available free of charge at https://pubs.acs.org/doi/10.1021/acscentsci.1c00906.

> Material synthesis; characterization details; IR, NMR, XPS; DFT calculations; and supporting figures (PDF)
> Crystallographic data for **3(UO$_2$)** (CIF)

AUTHOR INFORMATION

Corresponding Authors

Qi Sun − *Department of Chemistry, University of South Florida, Tampa, Florida 33620, United States;* ● orcid.org/0000-0002-1698-8741; Email: sunqichs@zju.edu.cn

Shengqian Ma − *Department of Chemistry, University of North Texas, Denton, Texas 76201, United States;* ● orcid.org/0000-0002-1897-7069; Email: shengqian.ma@unt.edu

Authors

Yanpei Song − *Department of Chemistry, University of North Texas, Denton, Texas 76201, United States*

Changjia Zhu − *Department of Chemistry, University of North Texas, Denton, Texas 76201, United States*

Briana Aguila − *Department of Chemistry, Francis Marion University, Florence, South Carolina 29506, United States*

Carter W. Abney − *ExxonMobil Research and Engineering Company, Annandale, New Jersey 08801, United States;* ● orcid.org/0000-0002-1809-9577

Lukasz Wojtas − *Department of Chemistry, University of South Florida, Tampa, Florida 33620, United States*

Complete contact information is available at:
https://pubs.acs.org/10.1021/acscentsci.1c00906

Notes

The authors declare no competing financial interest.

REFERENCES

(1) Taylor, R. Reaction: A role for actinide chemists. *Chem.* **2016**, *1*, 662−663.

(2) Gilbert, A. Q.; Bazilian, M. D. Can. dstributed nuclear power address energy resilience and energy poverty? *Joule* **2020**, *4*, 1839−1851.

(3) Deutch, J. Is net zero carbon 2050 possible? *Joule* **2020**, *4*, 2237−2243.

(4) Dresselhaus, M. S.; Thomas, I. L. Alternative energy technologies. *Nature* **2001**, *414*, 332−337.

(5) Dai, S. Catalyst: Challenges in development of adsorbents for recovery of uranium from seawater. *Chem.* 2021, 7, 537−539.

(6) Sun, Q.; Aguila, B.; Ma, S. Opportunities of porous organic polymers for radionuclide sequestration. *Trends Chem.* 2019, 1, 292−303.

(7) Zhang, H.; Liu, W.; Li, A.; Zhang, D.; Li, X.; Zhai, F.; Chen, L.; Chen, L.; Wang, Y.; Wang, S. Three mechanisms in one material: uranium capture by a polyoxometalate-organic framework through combined complexation, chemical reduction, and photocatalytic reduction. *Angew. Chem., Int. Ed.* 2019, 58, 16110−16114.

(8) Cui, W.-R.; Zhang, C.-R.; Jiang, W.; Li, F.-F.; Liang, R.-P.; Liu, J.; Qiu, J.-D. Regenerable and stable sp² carbon-conjugated covalent organic frameworks for selective detection and extraction of uranium. *Nat. Commun.* 2020, 11, 436.

(9) Yuan, Y.; Feng, S.; Feng, L.; Yu, Q.; Liu, T.; Wang, N. A bio-inspired nano-pocket spatial structure for targeting uranyl capture. *Angew. Chem., Int. Ed.* 2020, 59, 4262−4268.

(10) Sun, Q.; Aguila, B.; Earl, L. D.; Abney, C. W.; Wojtas, L.; Thallapally, P. K.; Ma, S. Covalent organic frameworks as a decorating platform for utilization and affinity enhancement of chelating sites for radionuclide sequestration. *Adv. Mater.* 2018, 30, 1705479.

(11) Yang, H.; Luo, M.; Luo, L.; Wang, H.; Hu, D.; Lin, J.; Wang, X.; Wang, Y.; Wang, S.; Bu, X.; Feng, P.; Wu, T. Highly selective and rapid uptake of radionuclide cesium based on robust zeolitic chalcogenide via stepwise ion-exchange strategy. *Chem. Mater.* 2016, 28, 8774−8780.

(12) Abney, C. W.; Mayes, R. T.; Saito, T.; Dai, S. Materials for the recovery of uranium from seawater. *Chem. Rev.* 2017, 117, 13935−14013.

(13) Tsouris, C. Fuel from seawater. *Nat. Energy* 2017, 2, 17022.

(14) Lu, Y. Uranium extraction: coordination chemistry in the ocean. *Nat. Chem.* 2014, 6, 175−177.

(15) Liu, C.; Hsu, P.-C.; Xie, J.; Zhao, J.; Wu, T.; Wang, H.; Liu, W.; Zhang, J.; Chu, S.; Cui, Y. A half-wave rectified alternating current electrochemical method for uranium extraction from seawater. *Nat. Energy* 2017, 2, 17007.

(16) Carboni, M.; Abney, C. W.; Liu, S.; Lin, W. Highly porous and stable metal-organic frameworks for uranium extraction. *Chem. Sci.* 2013, 4, 2396−2402.

(17) Zhou, L.; Bosscher, M.; Zhang, C.; Özçubukçu, S.; Zhang, L.; Zhang, W.; Li, C. J.; Liu, J.; Jensen, M. P.; Lai, L.; He, C. A protein engineered to bind uranyl selectively and with femtomolar affinity. *Nat. Chem.* 2014, 6, 236−241.

(18) Ma, S.; Huang, L.; Ma, L.; Shim, Y.; Islam, S. M.; Wang, P.; Zhao, L.-D.; Wang, S.; Sun, G.; Yang, X.; Kanatzidis, M. G. Efficient uranium capture by polysulfide/layered double hydroxide composites. *J. Am. Chem. Soc.* 2015, 137, 3670−3677.

(19) Ling, L.; Zhang, W.-x. Enrichment and encapsulation of uranium with iron nanoparticle. *J. Am. Chem. Soc.* 2015, 137, 2788−2791.

(20) Yuan, Y.; Niu, B.; Yu, Q.; Guo, X.; Guo, Z.; Wen, J.; Liu, T.; Zhang, H.; Wang, N. Photoinduced multiple effects to enhance uranium extraction from natural seawater by black phosphorus nanosheets. *Angew. Chem., Int. Ed.* 2020, 59, 1220−1227.

(21) Li, N.; Yang, L.; Wang, D.; Tang, C.; Deng, W.; Wang, Z. High-capacity amidoxime functionalized β-cyclodextrin/graphene aerogel for selective uranium capture. *Environ. Sci. Technol.* 2021, 55, 9181−9188.

(22) Sholl, D. S.; Lively, R. P. Seven chemical separations to change the world. *Nature* 2016, 532, 435−437.

(23) Parker, B. F.; Zhang, Z.; Rao, L.; Arnold, J. An overview and recent progress in the chemistry of uranium extraction from seawater. *Dalton Trans.* 2018, 47, 639−644.

(24) Wang, Z.; Meng, Q.; Ma, R.; Wang, Z.; Yang, Y.; Sha, H.; Ma, X.; Ruan, X.; Zou, X.; Yuan, Y.; Zhu, G. Constructing an ion pathway for uranium extraction from seawater. *Chem.* 2020, 6, 1−9.

(25) Yan, B.; Ma, C.; Gao, J.; Yuan, Y.; Wang, N. An ion-crosslinked supramolecular hydrogel for ultrahigh and fast uranium recovery from seawater. *Adv. Mater.* 2020, 32, 1906615.

(26) Chen, Z.; Chen, W. Y.; Jia, D. S.; Liu, Y.; Zhang, A. R.; Wen, T.; Liu, J.; Ai, Y. J.; Song, W. G.; Wang, X. K. N, P, and S codoped graphene-like carbon nanosheets for ultrafast uranium (VI) capture with high capacity. *Adv. Sci.* 2018, 5, 1800235.

(27) Kou, S.; Yang, Z.; Sun, F. Protein hydrogel microbeads for selective uranium mining from seawater. *ACS Appl. Mater. Interfaces* 2017, 9, 2035−2039.

(28) Piechowicz, M.; Abney, C. W.; Thacker, N. C.; Gilhula, J. C.; Wang, Y.; Veroneau, S. S.; Hu, A.; Lin, W. Successful coupling of a bis-amidoxime uranophile with a hydrophilic backbone for selective uranium sequestration. *ACS Appl. Mater. Interfaces* 2017, 9, 27894−27904.

(29) Macerata, E.; Mossini, E.; Scaravaggi, S.; Mariani, M.; Mele, A.; Panzeri, W.; Boubals, N.; Berthon, L.; Charbonnel, M.-C.; Sansone, F.; Arduini, A.; Casnati, A. Hydrophilic clicked 2,6-bis-triazolyl-pyridines endowed with high actinide selectivity and radiochemical stability: towards a closed nuclear fuel cycle. *J. Am. Chem. Soc.* 2016, 138, 7232−7235.

(30) Yuan, Y.; Yu, Q.; Cao, M.; Feng, L.; Feng, S.; Liu, T.; Feng, T.; Yan, B.; Guo, Z.; Wang, N. Selective extraction of uranium from seawater with biofouling-resistant polymeric peptide. *Nat. Sustain.* 2021, 4, 708.

(31) Yuan, Y.; Yang, Y.; Ma, X.; Meng, Q.; Wang, L.; Zhao, S.; Zhu, G. Molecularly imprinted porous aromatic frameworks and their composite components for selective extraction of uranium ions. *Adv. Mater.* 2018, 30, 1706507.

(32) Wang, X.-F.; Chen, Y.; Song, L.-P.; Fang, Z.; Zhang, J.; Shi, F.; Lin, Y.-W.; Sun, Y.; Zhang, Y.-B.; Rocha, J. Cooperative capture of uranyl ions by a carbonyl-bearing hierarchical-porous Cu-organic framework. *Angew. Chem., Int. Ed.* 2019, 58, 18808−18812.

(33) Yuan, Y.; Yu, Q.; Wen, J.; Li, C.; Guo, Z.; Wang, X.; Wang, N. Ultrafast and highly selective uranium extraction from seawater by hydrogel-like spidroin-based protein fiber. *Angew. Chem., Int. Ed.* 2019, 58, 11785−11790.

(34) Yuan, Y.; Liu, T.; Xiao, J.; Yu, Q.; Feng, L.; Niu, B.; Feng, S.; Zhang, J.; Wang, N. DNA nano-pocket for ultra-selective uranyl extraction from seawater. *Nat. Commun.* 2020, 11, 5708.

(35) Ivanov, A. S.; Parker, B. F.; Zhang, Z.; Aguila, B.; Sun, Q.; Ma, S.; Jansone-Popova, S.; Arnold, J.; Mayes, R. T.; Dai, S.; Bryantsev, V. S.; Rao, L.; Popovs, I. Siderophore-inspired chelator hijacks uranium from aqueous medium. *Nat. Commun.* 2019, 10, 819.

(36) Yu, B.; Zhang, L.; Ye, G.; Liu, Q.; Li, J.; Wang, X.; Chen, J.; Xu, S.; Ma, S. De novo synthesis of bifunctional conjugated microporous polymers for synergistic coordination mediated uranium entrapment. *Nano Res.* 2021, 14, 788−796.

(37) Sun, Q.; Song, Y.; Aguila, B.; Ivanov, A. S.; Bryantsev, V. S.; Ma, S. Spatial engineering direct cooperativity between binding sites for uranium sequestration. *Adv. Sci.* 2021, 8, 2001573.

(38) Feng, L.; Wang, H.; Feng, T.; Yan, B.; Yu, Q.; Zhang, J.; Guo, Z.; Yuan, Y.; Ma, C.; Liu, T.; Wang, N. In-situ synthesis of uranyl-imprinted nanocage for selective uranium recovery from seawater. *Angew. Chem., Int. Ed.* 2021, 60, DOI: 10.1002/anie.202101015.

(39) Li, Z.; Meng, Q.; Yang, Y.; Zou, X.; Yuan, Y.; Zhu, G. Constructing amidoxime-modified porous adsorbents with open architecture for cost-effective and efficient uranium extraction. *Chem. Sci.* 2020, 11, 4747−4752.

(40) Abney, C. W.; Mayes, R. T.; Piechowicz, M.; Lin, Z.; Bryantsev, V. S.; Veith, G. M.; Dai, S.; Lin, W. XAFS investigation of polyamidoxime-bound uranyl contests the paradigm from small molecule studies. *Energy Environ. Sci.* 2016, 9, 448−453.

(41) Ivanov, A. S.; Leggett, C. J.; Parker, B. F.; Zhang, Z.; Arnold, J.; Dai, S.; Abney, C. W.; Bryantsev, V. S.; Rao, L. Origin of the unusually strong and selective binding of vanadium by polyamidoximes in seawater. *Nat. Commun.* 2017, 8, 1560.

(42) Xu, X.; Zhang, H.; Ao, J.; Xu, L.; Liu, X.; Guo, X.; Li, J.; Zhang, L.; Li, Q.; Zhao, X.; Ye, B.; Wang, D.; Shen, F.; Ma, H. 3D hierarchical porous amidoxime fibers speed up uranium extraction from seawater. *Energy Environ. Sci.* 2019, 12, 1979−1988.

(43) Leggett, C. J.; Parker, B. F.; Teat, S. J.; Zhang, Z.; Dau, P. D.; Lukens, W. W.; Peterson, S. M.; Cardenas, A. J. P.; Warner, M. G.; Gibson, J. K.; Arnold, J.; Rao, L. Structural and spectroscopic studies of a rare non-oxido V(V) complex crystallized from aqueous solution. *Chem. Sci.* **2016**, *7*, 2775−2786.

(44) Sahiner, N.; Yu, H.; Tan, G.; He, J.; John, V. T.; Blake, D. A. Highly porous acrylonitrile-based submicron particles for UO_2^{2+} absorption in an immunosensor assay. *ACS Appl. Mater. Interfaces* **2012**, *4*, 163−170.

(45) Ivanov, A. S.; Bryantsev, V. S. Assessing ligand selectivity for uranium over vanadium ions to aid in the discovery of superior adsorbents for extraction of UO_2^{2+} from seawater. *Dalton Trans.* **2016**, *45*, 10744−10751.

(46) Yue, Y.; Mayes, R. T.; Kim, J.; Fulvio, P. F.; Sun, X.-G.; Tsouris, C.; Chen, J.; Brown, S.; Dai, S. Seawater uranium sorbents: preparation from a mesoporous copolymer initiator by atom-transfer radical polymerization. *Angew. Chem., Int. Ed.* **2013**, *52*, 13458−13462.

(47) Li, B.; Sun, Q.; Zhang, Y.; Abney, C.; Aguila, B.; Lin, W.; Ma, S. Functionalized Porous Aromatic Framework for Efficient Uranium Adsorption from Aqueous Solutions. *ACS Appl. Mater. Interfaces* **2017**, *9*, 12511−12517.

(48) Cui, W.-R.; Li, F.-F.; Xu, R.-H.; Zhang, C.-R.; Chen, X.-R.; Yan, R.-H.; Liang, R.-P.; Qiu, J.-D. Regenerable covalent organic frameworks for photo-enhanced uranium adsorption from seawater. *Angew. Chem., Int. Ed.* **2020**, *59*, 17684−17690.

(49) Yuan, Y.; Meng, Q.; Faheem, M.; Yang, Y.; Li, Z.; Wang, Z.; Deng, D.; Sun, F.; He, H.; Huang, Y.; Sha, H.; Zhu, G. A molecular coordination template strategy for designing selective porous aromatic framework materials for uranyl capture. *ACS Cent. Sci.* **2019**, *5*, 1432−1439.

(50) Yu, J.; Yuan, L.; Wang, S.; Lan, J.; Zheng, L.; Xu, C.; Chen, J.; Wang, L.; Huang, Z.; Tao, W.; Liu, Z.; Chai, Z.; Gibson, J. K.; Shi, W. Phosphonate-decorated covalent organic frameworks for actinide extraction: a breakthrough under highly acidic conditions. *CCS Chem.* **2019**, *1*, 286−295.

(51) Zhang, L.; Ye, G.; Pu, N.; Yu, B.; Chen, J.; Xu, S.; Ma, S. Skeleton Engineering of Homo-Coupled Conjugated Microporous Polymers for Highly Efficient Uranium Capture via Synergistic Coordination. *ACS Appl. Mater. Interfaces* **2020**, *12*, 3688−3696.

(52) Aguila, B.; Sun, Q.; Cassady, H.; Abney, C. W.; Li, B.; Ma, S. Design strategies to enhance amidoxime chelators for uranium recovery. *ACS Appl. Mater. Interfaces* **2019**, *11*, 30919−30926.

(53) Sun, Q.; Zhu, L.; Aguila, B.; Thallapally, P. K.; Xu, C.; Chen, J.; Wang, S.; Rogers, D.; Ma, S. Optimizing radionuclide sequestration in anion nanotraps with record pertechnetate sorption. *Nat. Commun.* **2019**, *10*, 1646.

(54) Aguila, B.; Sun, Q.; Cassady, H. C.; Shan, C.; Liang, Z.; Al-Enizic, A. M.; Nafadyc, A.; Wright, J. T.; Meulenberg, R. W.; Ma, S. A porous organic polymer nanotrap for efficient extraction of palladium. *Angew. Chem., Int. Ed.* **2020**, *59*, 19618−19622.

(55) Kelley, S. P.; Barber, P. S.; Mullins, P. H. K.; Rogers, R. D. Structural clues to UO_2^{2+}/VO_2^+ competition in seawater extraction using amidoxime-based extractants. *Chem. Commun.* **2014**, *50*, 12504−12507.

(56) Sun, Q.; Aguila, B.; Perman, J.; Ivanov, A. S.; Bryantsev, V. S.; Earl, L. D.; Abney, C. W.; Wojtas, L.; Ma, S. Bio-inspired nano-traps for uranium extraction from seawater and recovery from nuclear waste. *Nat. Commun.* **2018**, *9*, 1644.

(57) Sun, M.-H.; Huang, S.-Z.; Chen, L.-H.; Li, Y.; Yang, X.-Y.; Yuan, Z.-Y.; Su, B.-L. Applications of hierarchically structured porous materials from energy storage and conversion, catalysis, photo-catalysis, adsorption, separation, and sensing to biomedicine. *Chem. Soc. Rev.* **2016**, *45*, 3479−3563.

(58) Sun, Q.; Dai, Z.; Meng, X.; Xiao, F.-S. Porous polymer catalysts with hierarchical structures. *Chem. Soc. Rev.* **2015**, *44*, 6018−6034.

(59) Zhao, S.; Yuan, Y.; Yu, Q.; Niu, B.; Liao, J.; Guo, Z.; Wang, N. A dual-surface amidoximated halloysite nanotube for high-efficiency economical uranium extraction from seawater. *Angew. Chem., Int. Ed.* **2019**, *58*, 14979−14985.

(60) Das, S.; Brown, S.; Mayes, R. T.; Janke, C. J.; Tsouris, C.; Kuo, L. J.; Gill, G.; Dai, S. Novel poly(imide dioxime) sorbents: Development and testing for enhanced extraction of uranium from natural seawater. *Chem. Eng. J.* **2016**, *298*, 125−135.